



## Big Data Supports Image Format Conversion with Computer-Aided Graphic Design

Jitao Yan 

School of Surveying and Urban Spatial Information, Henan University of Urban Construction, Pingdingshan, Henan 467036, China, [yjt@huuc.edu.cn](mailto:yjt@huuc.edu.cn)

Corresponding author: Jitao Yan, [yjt@huuc.edu.cn](mailto:yjt@huuc.edu.cn)

**Abstract.** Image format conversion is an essential link in graphic design. The traditional image format conversion method will reduce image quality and low efficiency, so it can not meet the needs of designers. Therefore, this paper constructs the image format transformation and graphic design model based on a deep learning algorithm with the support of big data. The model improves the extraction of image feature information and non-critical information through CNN and attention mechanism, and the image compression quality is improved through the GAN model to optimize the image quality of the final format conversion. The experimental results show that compared with other models, the proposed model has better image quality index results and can provide better image quality and better stability under the same bit rate. The experimental results show that in practical application, the model can ensure that the graphic design can maintain a higher similarity with the original graphic design after format conversion, make it more in line with the designer's expectations, and provide better technical support for graphic design image format conversion.

**Keywords:** Big Data; Format Conversion; Computer Aided; Graphic Design

**DOI:** <https://doi.org/10.14733/cadaps.2025.S9.294-307>

### 1 INTRODUCTION

The wide application of big data technology provides new technical support for graphic design and broadens its development space. In previous graphic design, different image formats have different characteristics and limitations, such as colour depth, resolution, compression ratio, etc. [1]. These characteristics directly affect the choice and limitation of the designer in the graphic design process. At the same time, the image format determines the final output effect of the design work and also has a direct impact on the file transmission speed and storage efficiency [2]. Therefore, the designer needs to choose the appropriate image format according to the design purpose and output device. This makes the process of graphic design difficult, as designers need to face many different formats of image materials. Although traditional image formats, such as JPEG, PNG, GIF, etc., each have their unique advantages and scope of application, their inherent

limitations have gradually emerged in the context of today's explosive data growth [3]. On the one hand, the conversion between different formats usually requires the help of professional software tools, which are often based on complex encoding and decoding algorithms, and the conversion process is time-consuming and requires high hardware resources, especially for images with high resolution and high colour depth, and conversion efficiency becomes the bottleneck [4]. On the other hand, the traditional format has shortcomings in supporting the features of emerging technologies (such as transparency, animation effect, HDR, etc.), and it is difficult to meet the diversified and personalized design needs [5]. Therefore, how to improve the efficiency and quality of image format conversion through computer-aided technology and big data technology has become an important research content in the field of graphic design.

In the field of graphic design, although computer-aided design technology and graphic design software have greatly improved the work efficiency of designers, they still face difficulties in stimulating design creativity, accurately capturing market demand and automating optimal design [6]. Image format conversion can provide new development ideas for graphic design. Through image format conversion, designers can achieve a variety of creative effects. For example, different image formats and coding methods are used to create unique visual styles and colour effects [7]. According to the customer's needs and preferences, the image is converted to a specific format and size to meet the needs of individual customization. This helps to enhance the pertinence and attractiveness of design works [8]. In the graphic design process, image format conversion can be integrated seamlessly with other design tools and workflows as part of automated processing to achieve rapid output and release of design works [9]. However, traditional image format conversion often relies on complex encoding and decoding algorithms, which consume a large number of computing resources when processing images with high resolution and high colour depth, resulting in a time-consuming and inefficient conversion process. Many conversion processes require manual parameter setting or adjustment, which not only increases the complexity of the transformation but also limits the degree of automation of the transformation. During the conversion process, due to the different compression algorithms and encoding methods between different formats, pixel loss, and colour distortion may be caused, thus reducing the image quality. Traditional conversion methods often lack intelligent optimization mechanisms, which cannot automatically adjust the conversion parameters according to the image content to achieve the best conversion effect. Therefore, this paper builds an image format conversion and graphic design model with the support of big data combined with a deep learning algorithm [10]. The model improves the extraction quality of image key feature information through a convolutional neural network (CNN), retains more information elements, and provides more data support for image reconstruction. At the same time, the model also introduces a generative adversarial network (GAN) based on image format transformation to improve the quality of graphic design and rendering effect.

With the rapid development of big data technology, its application in image processing and analysis is becoming increasingly widespread. The image format conversion supported by big data can optimize conversion algorithms based on the analysis of massive image data, achieving more efficient and accurate format conversion [11]. Applying the CCPF method to the process of image format conversion can further improve the quality of the converted image. After conversion, use CCPF or similar image enhancement techniques again to perform post-processing on the conversion results, ensuring that the image still maintains high colour accuracy and detail richness after conversion. In computer-aided graphic design, image format conversion is a fundamental and critical process that not only affects the efficiency of file storage but also directly impacts the quality and performance of images in subsequent processing, transmission, and display [12]. These strategies can automatically adjust parameters such as colour correction, contrast enhancement, and detail preservation during the conversion process for specific types of images (such as underwater images), thereby achieving efficient format conversion while maintaining image quality. The big data platform can collect and analyze underwater image data from different sources, depths, and environmental conditions and identify the optimal conversion parameters and strategies between different image formats through machine learning algorithms. Specifically,

before conversion, the CCPF method can be used for image preprocessing to correct color cast and contrast reduction in underwater images caused by light scattering and selective attenuation. During the conversion process, optimize the conversion parameters by combining the conversion strategy of big data analysis. This image format conversion method that combines big data and advanced image processing technology has broad application prospects in fields such as ocean exploration, underwater archaeology, and underwater engineering monitoring. It can not only improve the processing efficiency and quality of underwater images, but also provide more reliable data support for advanced visual tasks such as image analysis, object recognition, and 3D reconstruction.

## 2 RELATED WORK

Image format conversion technology is a key component in the fields of computer vision and image processing. Its development not only promotes efficient storage and transmission of images but also promotes the widespread application of multimedia content. With the continuous advancement of technology, image format conversion technology has evolved from simple pixel-level operations to complex systems based on deep learning and advanced compression algorithms. Early image format conversion mainly relied on pixel-level operations, such as simple conversions between JPEG, PNG, and other formats. These conversions typically do not involve complex image processing algorithms but are based on file format encoding and decoding rules. As a widely used image compression format, JPEG achieves efficient image compression through discrete cosine transform (DCT) and quantization techniques. However, during the compression process, a certain amount of image quality will be lost, and transparency and animation will not be supported. With the rise of edge computing technology, image format conversion technology has begun to develop in the direction of real-time and efficiency. Edge computing reduces data transmission delay and bandwidth consumption through image processing on the device side and improves the user experience. For example, in an autonomous vehicle, Ma et al. [13] analyzed that image recognition and conversion technology can process images captured by onboard cameras in real time to provide accurate road information and obstacle detection for vehicles. The development of intelligent technology has opened up a technological space for image format conversion.

Miranda et al. [14] introduced convolutional neural networks into image style conversion, extracting content and style features of images through pre-trained CNN models. By optimizing the loss function, the style of one image is transformed into another image, thereby achieving the transformation of image style. It can apply different styles to ordinary landscape photos, creating unique works of art. On this basis, Tiancheng and Tieyi [15] introduced optimization algorithms to improve the performance of CNN models, giving them stronger generalization ability and better results and enabling them to achieve bidirectional conversion between two different styles of images. In addition to the above algorithms, the evolution of image formats has also promoted the development of conversion technology. As an emerging image format based on AV1 video codec, AVIF is gradually replacing traditional formats such as JPEG with its excellent compression efficiency and wide colour support. AVIF not only supports lossy and lossless compression but also processes transparency and HDR colours, with compression efficiency about 50% higher than JPEG. The promotion and application of AVIF have made image format conversion technology not limited to simple format conversion but also involve improving image quality and optimizing storage space. With the continuous innovation of technology and the expansion of application scenarios, image format conversion will further improve the accuracy and efficiency of conversion in future development, better handle image conversion in complex scenes, and solve compatibility issues between different devices.

To further improve the accuracy of image quality assessment, Wang et al. [16] combined the spatial average of feature maps (representing texture similarity) with the correlation of feature maps themselves (representing structural similarity) to construct a comprehensive image quality measurement method. In model construction, we use Convolutional Neural Networks (CNN) to

extract multi-scale overcomplete representations of images. This representation not only captures the local features of the image but also reveals the global structure and texture patterns of the image through fusion at different scales. Specifically, Wang et al. [17] found that the spatial averages of feature maps in these representations can effectively reflect the appearance of textures, as they provide sufficient statistical constraints to simulate and recognize multiple texture patterns. This method can not only evaluate the fidelity of images in the global structure but also sensitively capture subtle changes in texture regions, thereby achieving better quality preservation during image format conversion. The experimental results show that the optimized model performs well on both traditional image quality databases and specialized texture databases, and can accurately explain human perceptual scores. This discovery provides a solid theoretical basis for maintaining texture quality during image format conversion. In addition, the model also provides competitive performance in tasks such as texture classification and retrieval, demonstrating its broad application potential. Using a big data platform, joint optimization of model parameters is carried out to maximize the matching of human evaluations of image quality and minimize the reporting distance between sub-images cropped from the same texture image.

With the rapid development of big data technology, Yi [18] has made significant progress in the research of PCNN-based models in the field of image processing. In terms of image format conversion, PCNN's excellent information extraction and processing capabilities demonstrate enormous potential. Traditional image format conversion methods often rely on fixed algorithms or rules, making it difficult to adapt to complex and ever-changing image content. The support of big data provides abundant data resources for the training and optimization of PCNN models, enabling them to learn more complex and subtle image features, thereby further improving their performance. In addition, PCNN can also preserve important structural and texture information of the image during the conversion process, ensuring the quality of the converted image is effectively guaranteed. These studies not only focus on reducing the number of manual parameters to achieve simulations that are closer to real cortical functions but also actively explore ways to combine PCNN with other advanced methods. The PCNN model can automatically adjust and optimize conversion parameters by learning image features from big data, achieving more accurate and efficient format conversion. Specifically, the application of PCNN in image format conversion can include the following aspects. One is to optimize the parameter settings during the encoding and decoding process, reduce data loss, maintain image clarity, and achieve high-quality image compression and decompression. Secondly, it supports the mutual conversion of multiple image formats, such as from JPEG to PNG or from RAW to JPEG, to meet the needs of different application scenarios. The third is to select image quality levels and compression ratios intelligently, balance transmission speed and image quality, and optimize bandwidth usage during image transmission.

### **3 IMAGE FORMAT CONVERSION AND GRAPHIC DESIGN MODEL BASED ON DEEP LEARNING**

#### **3.1 Image Format Conversion Module Based on Convolutional Neural Network**

In image format conversion, CNN can automatically learn from the original image data and extract useful features, such as edges, textures, shapes, etc. These features are crucial for image format conversion because they capture the image's essential properties, helping preserve key information about the image during the conversion process. Using multiple convolutional layers and nonlinear activation layers, CNN can gradually abstract the high-level features of images. These advanced features not only contain the image's local details but also the global semantic information, which provides a rich information source for image format conversion. In the process of image format conversion, maintaining the consistency of image content is key. By learning the deep representation of the image content, CNN can keep the main content and structure of the image unchanged as much as possible during the conversion process to ensure that the converted image is still recognizable and practical. Figure 1 shows the structure diagram of a convolutional neural network.

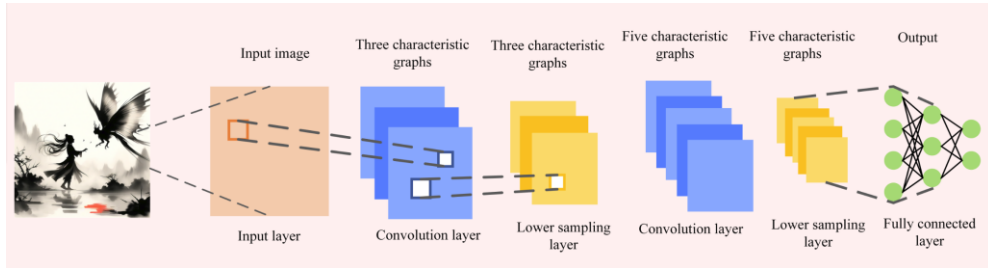


**Figure 1:** Structure diagram of convolutional neural network.

Compared with the fully connected structure commonly used in feedforward neural networks, CNN significantly introduces a sparse connection mechanism to achieve a regularization effect, effectively enhancing the robustness and generalization ability of the network structure and thus avoiding the risk of overfitting. At the same time, the sparse join strategy also greatly reduces the total number of parameters that the model needs to learn, significantly improves the efficiency of the training process, and reduces the demand for computing resources, especially memory. In addition, CNNs realizes the connection between adjacent neurons through the core component of the "convolutional kernel," and the parameter-sharing property of the convolutional kernel further reduces the size of the model, making training more efficient and resource-friendly. Let the input image be  $X$ , the Convolution kernel is  $K$  and the size is  $m * m$ , then the final output feature diagram is shown in formula (1):

$$Y_j(j \in p * q) = f\left(\sum_{i \in m * m} X_i * K_i + b\right) \quad (1)$$

In the formula, the bias quantity is expressed as  $b$  the final output graph size is shown as  $p * q$ .

Locate in  $L-1$  mid-layer control  $j$  the output feature map is represented  $a_j^{L-1}$ , after passing through the pooling layer, as shown in formula (2):

$$a_j^L = f(\text{down}(a_j^{L-1}) + b_j^L) \quad (2)$$

The amount of bias in the formula is expressed as  $b_j^L$  the pooling function  $\text{down}()$ .

The CNN activation function is shown in formula (3):

$$\text{relu}(x) = \max(0, x) \quad (3)$$

The loss function is shown in formula (4):

$$\text{loss}(Y, \hat{Y}) = \frac{1}{N} \sum_{i=1}^N (y_i - \hat{y}_i)^2 \quad (4)$$

Generalized Divisive Normalization (GDN) is used to enhance the model's stability and performance to normalize the feature data extracted by CNN. The calculation formulas of GDN and IGDN are shown in (5) and (6):

$$\text{textGDN}(x) = \frac{x}{\sqrt{\sum_j \gamma_{ij}(x_j^2 + \text{pedestal}) + \beta_i}} \quad (5)$$

$$\text{textIGDN}(x) = x \left[ \sum_j \gamma_{ij}(x_j^2 + \text{pedestal}) + \beta_i \right]^{\frac{1}{2}} \quad (6)$$

Different feature dimensions pass  $x$ ,  $i, j$  respectively, the weight matrix is expressed as  $\gamma_{ij}$ , and The offset is expressed as  $\beta_i$ .

In the field of graphic design, image details are required to be relatively high, that is, image presentation quality is high. Therefore, to improve the adequacy of the CNN model for feature processing and improve image reconstruction quality, this paper introduces a mixed attention mechanism, whose core goal is to strengthen the model's ability to capture and analyze local feature details. The mechanism cleverly introduces the shuffle operation, that is, by rearranging or reorganizing the local features of the input data, the original feature arrangement order is broken, so that the network is more sensitive to identify and distinguish between non-repetitive texture and redundant information. Figure 2 shows a schematic of the mixed attention mechanism.

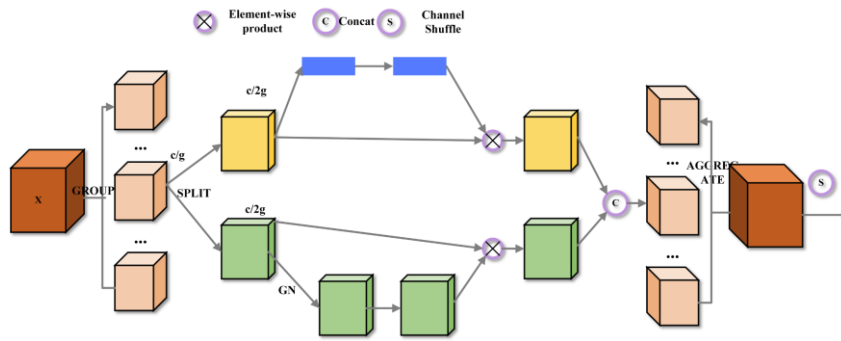


**Figure 2:** Schematic diagram of mixed attention mechanism.

The figure shows that the hybrid attention mechanism is composed of a channel attention module and a spatial attention module; channel attention is designed to model the correlation between different channels, strengthen the important features, and suppress the non-important features. Spatial attention is focused on improving the feature representation of key regions by weighting out target regions of interest and weakening background regions. Combining the two methods can form a more comprehensive feature attention method and enhance the model's ability to recognize key features. The final output of the channel attention module is shown in formula (7):

$$\begin{aligned}
 M_c(F) &= \sigma\{MLP[AvgPool(F)] + MLP[MaxPool(F)]\} \\
 &= \sigma\{MLP[\frac{1}{H+W} \sum_{n_0=1}^H \sum_{m_0=1}^W f_{x_0}(n_0, m_0)] + MLP[\max_{n \in H, m \in W} f_{x_0}(n, m)]\}
 \end{aligned}
 \tag{7}$$

Where the activation function is Sigmoid. It is expressed as  $\sigma$ , the height and width of the input feature map are expressed as  $H$  and  $W$ , input eigenvalues in sequence number  $x_0$  the coordinates in the channel are  $(n_0, m_0)$  the point corresponding to the pixel value is expressed as  $f_{x_0}(n_0, m_0)$ .

The spatial attention module expression is shown in (8):

$$M_s(F) = \sigma\{f^{k \times k}[AvgPool(F^i); MaxPool(F^i)]\}
 \tag{8}$$

Where the size of the convolution kernel is  $k \times k$  the convolution layer is represented by  $f^{k \times k}$ .

The final expression of the mixed attention mechanism is shown in (9):

$$\begin{cases}
 F^i = M_c \otimes F \\
 F^n = M_s \otimes F^i
 \end{cases}
 \tag{9}$$

Where the multiplication of the corresponding elements of the two matrices is expressed as  $\otimes$ .

### 3.2 Image Compression Module Based on Generative Adversarial Network

In the process of graphic design, designers often need to deal with a large number of image materials. Through image compression, the size of these image files can be significantly reduced, thus speeding up the opening, editing, and saving of files and improving the design efficiency. If the compressed image file can take up less storage space, the designer can manage the image resources in the design project more efficiently and avoid affecting the design schedule due to insufficient storage space. In addition, the quality of the compressed image also directly affects the final rendering effect of the graphic design. In this paper, an image compression module is constructed using the generative adversarial network to ensure the quality of the compressed graphic design. Figure 3 shows the schematic diagram of the image coding framework based on a generative adversarial network.

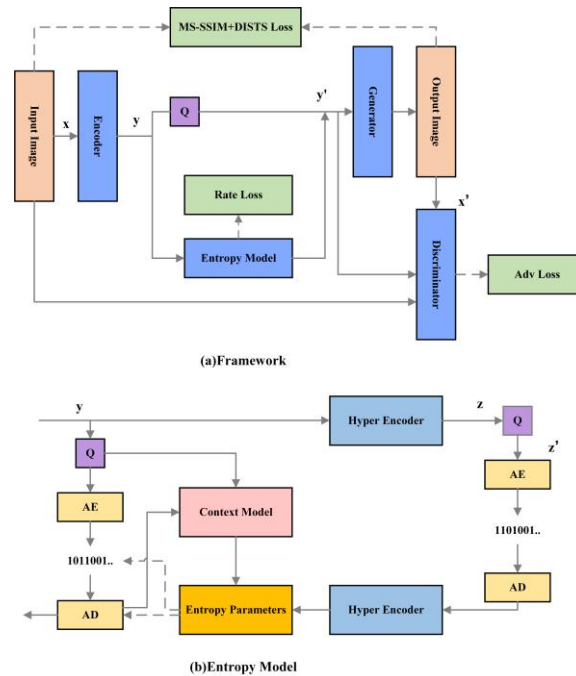


**Figure 3:** Schematic diagram of image coding framework based on generating adversarial network.

As can be seen from the figure, the input image will first obtain the corresponding potential representation through the encoder structure of the multi-layer convolutional structure  $y$ , in this process, after each layer of convolution operation, the channel normalization step is used to alleviate the artifacts generated in the coding process and improve the model performance. Later  $y$  it is quantified and timed to meet subsequent processing and image storage requirements. Also, before quantification

$y$  input into a complex entropy model to obtain the probability distribution of the corresponding part. In the process of image compression, the entropy model can quantify the amount of information in the image. The complexity and uncertainty of the image data can be understood by calculating the entropy value of the image. Images with high entropy usually contain more information and, therefore, require more bits to encode; Low-entropy images, on the other hand, are simpler and can be represented by fewer bits. The entropy model can also be used

to optimize parameter Settings during compression. By adjusting the parameters of the compression algorithm, the compressed image can have a smaller file size while maintaining a certain quality. The entropy model can also be used to evaluate the quality of compressed images. By comparing the entropy difference between the original image and the compressed image, we can judge the retention degree of the image information. In this paper, GLLMM probability estimation is adopted in the entropy model, and its description is shown in (10):

$$P_{y|\hat{z}}(y|\hat{z}) = [p_0 \sum_{k=1}^K N(\mu_i^{(k)}, \sigma_i^{2(k)}) + p_1 \sum_{m=1}^M \omega_i^m Lap(\mu_i^{(m)}, \sigma_i^{2(m)}) + p_2 \sum_{n=1}^N \omega_i^n Log(\mu_i^{(n)}, \sigma_i^{2(n)})] * U(-\frac{1}{2}, \frac{1}{2}) = c(y + \frac{1}{2}) - c(\hat{y}_l - \frac{1}{2}) \quad (10)$$

Where the uniform distribution is expressed as  $N()$ , the Laplace distribution is expressed as  $Lap()$ , The logical distribution is expressed as  $Log()$ , relevant parameters are  $p_i, \omega_i, \mu_i, \sigma_i$ , the cumulative function is expressed as  $c()$ , and the mean and variance are expressed as  $\mu, \sigma$ .

The objective function is shown in (11) and (12):

$$L_{E,H,G} = D(x, x) + \lambda(R(y) + R(z)) + \beta[D(\hat{x}, y) - 1]^2 \quad (11)$$

$$L_D = E_{x-pX}[D(\hat{x}, y) - 1]^2 + E_{x-pX}[D(x, y) - 1]^2 \quad (12)$$

Where the generator is represented as  $G$ , the discriminator is expressed as  $D$ , the core underlying representation is described as  $R(\hat{y})$  the edge information entropy is described as  $R(\hat{z})$  the distortion term is expressed as  $D(x, \hat{x})$ .

The output decoded by the entropy model is fed into a generator for image reconstruction, which contains residual blocks and deconvolution layers. The underlying representation, the original image, and the reconstructed image end up in a discriminator with five convolutional layers designed to improve the authenticity of the generator's output image. Table 1 shows the parameters related to the network structure.

<i>Encoder</i>	<i>Generator</i>	<i>Discriminator</i>
Conv 7×7×60 Norm	Norm Conv 960 Norm	Conv 12-NN 16
Conv 120 s2 Norm	ResBlock(×5):Conv 960 Norm	Conv 4×4×64 s2
Conv 240 s2 Norm	Conv 480 s2 Norm	Conv 4×4×128 s2
Conv 480 s2 Norm	Conv 240 s2 Norm	Conv 4×4×256 s2
Conv 960 s2 Norm	Conv 120 s2 Norm	Conv 4×4×512 s2
Conv 220	Conv 60 s2 Norm	Conv 1×1×1 Sigmoid
	Conv 7×7×3	

**Table 1:** Related information of image coding structure based on generating adversarial network.

## 4 EXPERIMENTAL RESULTS AND ANALYSIS OF IMAGE FORMAT CONVERSION AND GRAPHIC DESIGN MODEL BASED ON DEEP LEARNING

### 4.1 Selection of Experimental Indexes

The model experiment part includes the model performance test and its application in graphic design. The performance test is mainly to evaluate the quality of the model after image format conversion. The following evaluation indexes are selected in this paper.



PSNR is an image quality evaluation index based on mean square error (MSE), which is used to measure the quality of image reconstruction. Its calculation formula is shown in (13):

$$PSNR = 10 \times \log_{10} MAX^2 / MSE \quad (13)$$

Where the maximum pixel value of the image is described as  $MAX$  the root mean square error between the original image and the converted image is expressed as  $MSE$ .

SSIM is a more advanced image quality evaluation index, which not only considers the difference in pixel values but also considers the structural information of the image and tries to simulate the perception of the human visual system to the image quality. Its basic form is shown in (14):

$$SSIM(x, y) = \frac{(2\mu_x\mu_y + C_1)(2\sigma_{xy} + C_2)}{(\mu_x^2 + \mu_y^2 + C_1)(\sigma_x^2 + \sigma_y^2 + C_2)} \quad (14)$$

In the formula, the pixel value matrix of the two images is respectively expressed as  $x, y$  its mean is expressed  $\mu_x, \mu_y$  variance is expressed as  $\sigma_x^2, \sigma_y^2$  the covariance representing the structural similarity between them is expressed as  $\sigma_{xy}$  the constant is  $C_1, C_2$ .

LPIPS is a metric used to measure the perceptual similarity of two images, which more accurately reflects the visual similarity of an image because it takes into account higher-level features of the image, such as texture, edge, and colour distribution. Its expression is shown in (15):

$$LPIPS(x, y) = \sum_l \frac{1}{H_l W_l} \sum_{h,w} \|w_l \otimes (y_i^{hw} - \hat{x}_i^{hw})\|_2^2 \quad (15)$$

Where the number of layers of the network is expressed as  $l$  the corresponding height and width of the feature map are respectively expressed as  $H_l, W_l$ , the corresponding weight is expressed as  $w_l$ , the normalized eigenvector is expressed as  $y_i^{hw}, \hat{x}_i^{hw}$ .

FID is a metric used to evaluate the similarity between the generated image and the real image by calculating the distance between the generated image and the real image in the feature space.

$$FID = \|\mu_r - \mu_g\|_2^2 + Tr(\Sigma_r + \Sigma_g - 2(\Sigma_r \Sigma_g)^{\frac{1}{2}}) \quad (16)$$

Where the mean vectors of real and generated images in feature space are respectively expressed as  $\mu_r, \mu_g$ , the covariance matrix of the two is expressed as  $\Sigma_r, \Sigma_g$ .

KID measures the distance between the generated image set and the real image set in the Inception feature space.

The design idea of NIQE is based on constructing a series of features used to measure image quality and fitting these features into a multivariate Gaussian model. These features are usually extracted from some simple and highly regular images of natural landscapes. NIQE assesses the quality of an image by calculating the difference between the image to be tested and the distribution of these natural image features.

## 4.2 Experimental Results and Analysis

In image format conversion, the sampling rate is directly related to the acquisition density and accuracy of image data, and then affects the quality of image format conversion. A higher sampling rate means that more pixels can be captured per unit time, thus preserving more image detail. The sample rate also affects the image's ability to reproduce colour. The higher sampling

rate can capture the color information in the image more accurately so that the converted image is closer to the original image in color. Figure 4 shows the relationship curve between the number of iterations of the model and the value of the loss function under different sampling rates. The results show that the relationship between the number of iterations and the loss function is a negative correlation, which indicates that the model can realize self-optimization through learning in the process of continuous iteration. From the sampling rate condition, the higher the sampling rate, the faster the convergence rate and the lower the value of the curve. However, when the sampling rate is higher than 0.3, the value of the curve changes gradually. Therefore, considering the actual demand, the sampling rate of the model in this paper is 0.4.

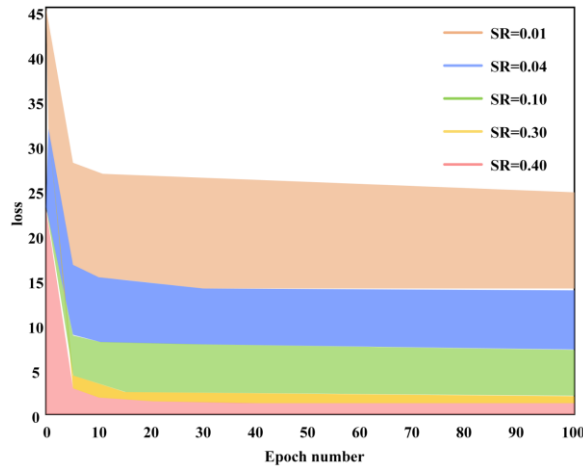


**Figure 4:** Relationship curve between iteration times and loss function values of the model under different sampling rates.

After determining the model parameters, the experiment selected another three commonly used image format conversion models as the control group to test the model performance. Figure 5 shows the comparison results of two sets of index values for four different models in the same test data set. Both of these indicators reflect the subjective quality of the image after format conversion, and the relationship between their values and quality is a negative correlation. LPIPS value results show that there are differences in the starting points of indicator curves of the four different models, among which the bit-rate value and the index value of the starting point of the grey image are relatively high, indicating that it not only require a higher transmission rate but also has poor image quality. The curves of the binary image and index image are close, and the two have lower requirements for transmission speed. Both values of the model curve in this paper are lower; that is, they can show better image quality under the condition of a lower transmission rate. In the FID value plot, the result is similar to the LPIPS value plot; the grey level image has the highest curve value, and there is a large gap between it and the other third model. The curve performance of the model in this paper is the best, which can ensure better image quality after conversion.

The comparison results of the KID and NIQE index curves of four different models are shown in Figure 6. These two indexes are also subjective quality evaluation indexes, but they are more capable of comprehensively evaluating image quality. The relationship between the two indexes and image quality presents a negative correlation. As can be seen from the KID index chart, the index values of the other three models all start from the highest point, but the requirements for the transmission rate are different, and the grey image still has the highest value. The curve starting point of the model in this paper is significantly lower than that of the other three models, which indicates that the image quality after conversion is better and the transmission rate is lower.

It can be seen from the NIQE index chart that the image quality of the grey-scale image is still in the lowest state among the four models, and the image quality of the model transformation in this paper has always maintained a high-quality state.

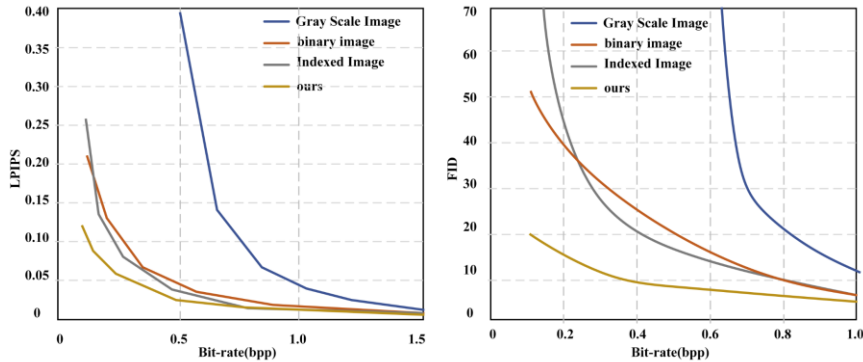


**Figure 5:** LPIPS and FID index values of four different models in the same test data set.

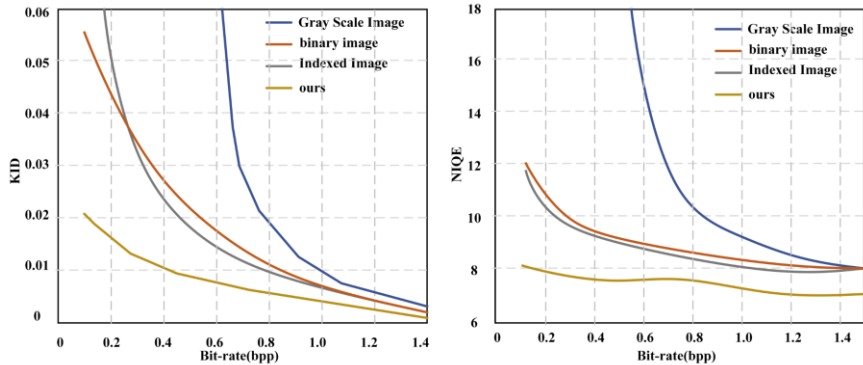


**Figure 6:** KID and NIQE index curves of four different models.

Figure 7 shows the comparison results of the PSNR and SSIM index curves of the four models. These two indicators can reflect the objective image quality, and the relationship between the two index values and image quality is a positive correlation. It can be seen from the results of the PSNR value that the image quality of this model is still significantly better than that of the other three models, and the image quality state is relatively stable. The SSIM index map shows that the image quality of the other three models is still lower than that of the model in this paper. Under the condition of a low bit rate, there is a large gap between the model, the binary image, and the index image. Under the condition of a high bit rate, the gap between the three is narrowed to a certain extent, and the quality of the model in this paper is slightly higher. It can be seen that the model in this paper has better performance among the four models, has better stability, and can provide better quality converted images in the practical application of graphic design.

To further test the application performance of the model in graphic design, this paper will analyze the definition, colour, resolution, spatial, and other aspects of the image format conversion and compare the model into a binary image and index image. Figure 8 shows the comparison results of image distortion after the conversion of the three models. It can be seen from the results that the design graphics after conversion of the binary image and the indexed image model have a certain degree of image distortion. On the one hand, there is room for tuning

model parameters; on the other hand, the two have weak performance in image reconstruction. The image converted by the model in this paper can maintain consistency with the original image and show better application performance.

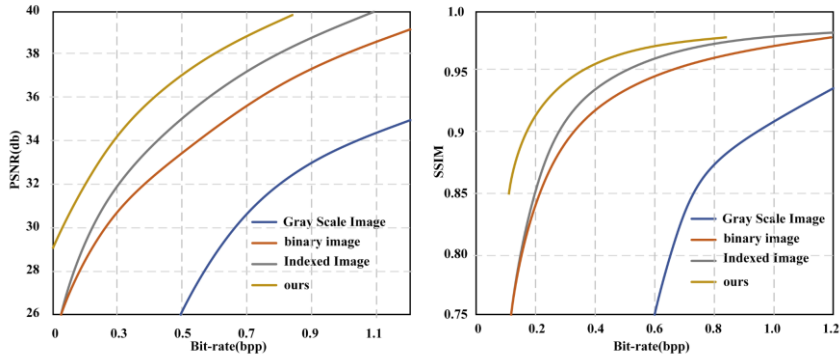


Figure 7: PSNR and SSIM index curves of four models.

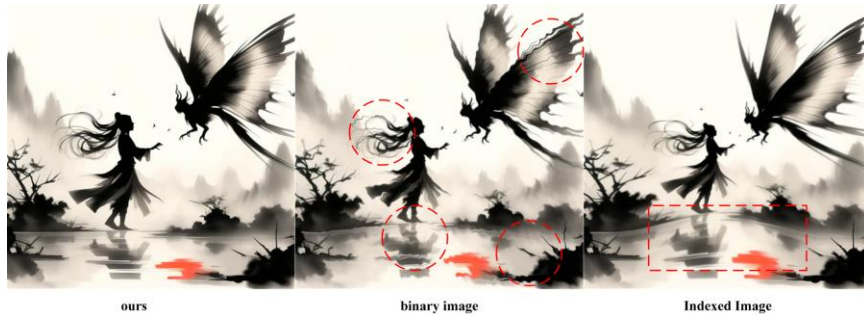


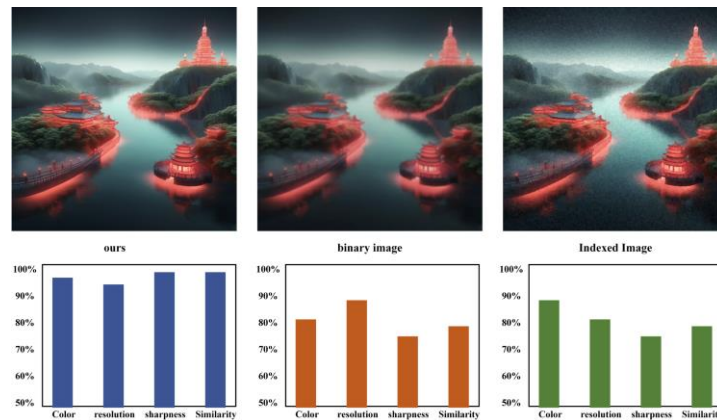
Figure 8: Comparison of image distortion after conversion of three models.

Figure 9 shows the quality comparison between the three models after the conversion of images with rich colours. The results show that the clarity of images after the conversion of binary images is relatively low, and the colour difference is the highest among the three images. The colour difference of the index image is maintained well, but the clarity and resolution are low, which cannot meet the requirements of a large display of the image. The values of all aspects of the image converted by the model in this paper are the highest, that is, the similarity between the image and the original image is the highest.

## 5 CONCLUSIONS

A large number of different image elements need to be used in the process of graphic design. If there is no format difference between image elements, designers need to carry out more image format conversions. The traditional image format conversion method is cumbersome and inefficient, and the quality of the converted image cannot meet the needs of designers. Therefore, this paper builds an image format conversion model based on big data support and deep learning algorithms. The CNN model is used to improve the quality of image feature extraction and conversion, and the GAN model is used to optimize the image compression performance of the model and finally ensure the quality of image format conversion. The experimental results show that compared with other models, the image index value of the proposed model is higher, and

there is an obvious gap, which shows better stability and can provide better image format conversion data for graphic design. The application experiment results show that the reconstructed image of this model is closer to the actual image in terms of image distortion, resolution, colour difference, clarity and other aspects, that is, it can retain more image details and display them in the process of format conversion, and can ensure that the graphic design can still meet the needs and requirements of designers after format conversion.



**Figure 9:** Comparison of the quality of the colourful image after conversion by three models.

## 6 ACKNOWLEDGEMENT

Henan Provincial Education Reform Project: Exploration and Practice of the "O2O" Operation and Management Model of Big Data Empowerment Application-oriented Undergraduate University Entrepreneurship Park, 2024SJGLX1102.

*Jitao Yan*, <https://orcid.org/0009-0000-2628-8346>

## REFERENCES

- [1] Adjabi, I.; Ouahabi, A.; Benzaoui, A.; Jacques, S.: Multi-block color-binarized statistical images for single-sample face recognition, *Sensors*, 21(3), 2021, 728. <https://doi.org/10.3390/s21030728>
- [2] Alfio, V.-S.; Costantino, D.; Pepe, M.: Influence of image TIFF format and JPEG compression level in the accuracy of the 3D model and quality of the orthophoto in UAV photogrammetry, *Journal of Imaging*, 6(5), 2020, 30. <https://doi.org/10.3390/jimaging6050030>
- [3] Amri, S.-Q.-S.; Ghani, A.-S.-A.; Baharin, M.-A.-S.-K.; Abu, M.-Y.; Fusaomi, N.: Improving images in turbid water through enhanced color correction and particle swarm-intelligence fusion (CCPF), *MEKATRONIKA*, 5(1), 2023, 18-35. <https://doi.org/10.15282/mekatronika.v5i1.9085>
- [4] Bhatt, J.; Hashmi, K.-A.; Afzal, M.-Z.; Stricker, D.: A survey of graphical page object detection with deep neural networks, *Applied Sciences*, 11(12), 2021, 5344. <https://doi.org/10.3390/app11125344>
- [5] Chen, S.: Exploration of artistic creation of Chinese ink style painting based on deep learning framework and convolutional neural network model, *Soft Computing*, 24(11), 2020, 7873-7884. <https://doi.org/10.1007/s00500-019-03985-6>
- [6] Ding, K.; Ma, K.; Wang, S.; Simoncelli, E.-P.: Image quality assessment: Unifying structure and texture similarity, *IEEE Transactions on Pattern Analysis and Machine Intelligence*, 44(5), 2020, 2567-2581. <https://doi.org/10.1109/TPAMI.2020.3045810>

- [7] Huo, J.; Yu, X.: Three-dimensional mechanical parts reconstruction technology based on a two-dimensional image, *International Journal of Advanced Robotic Systems*, 17(2), 2020, 1-11. <https://doi.org/10.1177/1729881420910008>
- [8] Jiang, H.; Yang, T.: Research on the extraction method of painting style features based on convolutional neural network, *International Journal of Arts and Technology*, 14(1), 2022, 40-55. <https://doi.org/10.1504/IJART.2022.122448>
- [9] Kantor, J.-M.: Polar format-based compressive SAR image reconstruction with integrated autofocus, *IEEE Transactions on Geoscience and Remote Sensing*, 58(5), 2019, 3458-3468. <https://doi.org/10.1109/TGRS.2019.2956432>
- [10] Li, Y.; Qi, Y.; Shi, Y.; Chen, Q.; Cao, N.; Chen, S.: Diverse interaction recommendation for public users exploring multi-view visualization using deep learning, *IEEE Transactions on Visualization and Computer Graphics*, 29(1), 2022, 95-105. <https://doi.org/10.1109/TVCG.2022.3209461>
- [11] Liu, H.; Liu, M.; Li, D.; Zheng, W.; Yin, L.; Wang, R.: Recent advances in pulse-coupled neural networks with applications in image processing, *Electronics*, 11(20), 2022, 3264. <https://doi.org/10.3390/electronics11203264>
- [12] Liu, X.; Li, N.; Xia, Y.: Affective image classification by jointly using interpretable art features and semantic annotations, *Journal of Visual Communication & Image Representation*, 58(1), 2019, 576-588. <https://doi.org/10.1016/j.jvcir.2018.12.032>
- [13] Ma, Y.; Xie, T.; Li, J.; Maciejewski, R.: Explaining vulnerabilities to adversarial machine learning through visual analytics, *IEEE Transactions on Visualization and Computer Graphics*, 26(1), 2019, 1075-1085. <https://doi.org/10.1109/TVCG.2019.2934631>
- [14] Miranda, V.-M.; Madlum, D.-V.; Oliveira, S.-N.; Gaêta, A.-H.; Haiter, N.-F.; Oliveira, M.-L.: Influence of the image file format of digital periapical radiographs on the diagnosis of external and internal root resorptions, *Clinical oral investigations*, 25(1), 2021, 4941-4948. <https://doi.org/10.1007/s00784-021-03803-0>
- [15] Tiancheng, Z.; Tiewi, C.: The preliminary study on the application of modern advanced processing technique in non-legacy cultural and creative product design-- Taking Wuhu iron painting as an example, *E3S Web of Conferences*, 179(3), 2020, 02091. <https://doi.org/10.1051/e3sconf/202017902091>
- [16] Wang, Q.; Xu, Z.; Chen, Z.; Wang, Y.; Liu, S.; Qu, H.: Visual analysis of discrimination in machine learning, *IEEE Transactions on Visualization and Computer Graphics*, 27(2), 2020, 1470-1480. <https://doi.org/10.1109/TVCG.2020.3030471>
- [17] Wang, Z.-J.; Turko, R.; Shaikh, O.; Park, H.; Das, N.; Hohman, F.; Chau, D.-H.-P.: CNN explainer: learning convolutional neural networks with interactive visualization, *IEEE Transactions on Visualization and Computer Graphics*, 27(2), 2020, 1396-1406. <https://doi.org/10.1109/TVCG.2020.3030418>
- [18] Yi, X.: DRIIS: Research on image classification of art education system based on deep learning, *International Journal of Cooperative Information Systems*, 31(01n02), 2022, 2150007. <https://doi.org/10.1142/S0218843021500076>